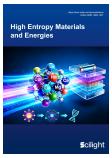
High Entropy Materials and Energies
https://www.sciltp.com/journals/heme



Review

Check for updates

Fission-Informed Partial/Local High-Entropy Design in Nuclear Ceramics: Opportunities and Constraints

Jiasheng Wang [1,2] and Yong Zhang [1,2,*]

[1] State Key Laboratory for Advanced Metals and Materials, University of Science and Technology Beijing, Beijing 100083, China
[2] Key Laboratory of Silicon-based Materials, Fujian Fuyao University of Science and Technology, Fuzhou 350109, China
* Correspondence: drzhangy@ustb.edu.cn

How To Cite: Wang, J.; Zhang, Y. Fission-Informed Partial/Local High-Entropy Design in Nuclear Ceramics: Opportunities and Constraints. *High Entropy Materials and Energies* **2026**, *1*(1), 6. https://doi.org/10.53941/heme.2026.100006

Received: 1 August 2026
Revised: 4 September 2026
Accepted: 23 September 2026
Published: 9 October 2026

Abstract: High-entropy ceramics are generally designed by distributing several principal cations over one or more crystallographic sublattices. Nuclear fuel ceramics develop a different form of chemical complexity: fission, neutron capture, radioactive decay, redox changes, temperature gradients, and diffusion produce a phase-partitioned UO_2 microstructure containing dissolved fission products, gas bubbles, noble-metal precipitates, complex oxides, and chemically modified interfaces. Here we use this irradiation-driven partitioning to motivate partial/local high-entropy (PLHE) design, in which deliberately introduced compositional complexity is confined to a function-controlling sublattice, grain-boundary region, interface, or secondary phase while the primary matrix is retained. Irradiated UO_2 is treated as a non-equilibrium heterogeneous state rather than a high-entropy phase. PLHE is defined by resolved spatial or crystallographic confinement, local compositional/site evidence, a specified performance bottleneck, and comparison with a matched lower-complexity reference. The resulting framework treats configurational entropy as one screening metric within broader thermodynamic and kinetic constraints. Waste-form ceramics provide the most direct near-term test bed, whereas fuel-matrix and in-fuel concepts require additional thermal, neutronic, redox, and irradiation screening.

Keywords: nuclear ceramics; UO_2 fuel; fission products; compositionally complex ceramics; partial/local high entropy; radiation tolerance

1. Introduction: High Entropy beyond Global Mixing

Configurational disorder has become an important design variable in ceramics. Rost et al. showed that the rock-salt oxide (Mg,Co,Ni,Cu,Zn)O could reversibly form a single phase at high temperature, providing direct evidence for entropy stabilization [1]. High-entropy ceramics have since been reported in fluorite, pyrochlore, perovskite, spinel, carbide, nitride, boride, and silicide systems [2–4]. The terminology has also been refined. A material may be compositionally complex without being entropy-stabilized, and a multicomponent nominal composition does not establish homogeneous mixing on a given sublattice or show that configurational entropy controls phase stability [5,6]. These distinctions are especially relevant to non-equimolar, aliovalent, vacancy-containing, ordered, and multiphase ceramics.

Studies of fluorite oxides show that medium-entropy and non-equimolar compositions can provide property combinations that equal or exceed those of equimolar analogues. Cation ordering, oxygen-vacancy content, local distortion, and phase stability can be as important as the number of components [7–9]. The design problem is therefore not to maximize configurational entropy throughout the material, but to determine where compositional complexity is useful and at what length scale.

Copyright: © 2026 by the authors. This is an open access article under the terms and conditions of the Creative Commons Attribution (CC BY) license (https://creativecommons.org/licenses/by/4.0/).
Publisher's Note: Scilight stays neutral with regard to jurisdictional claims in published maps and institutional affiliations.

Nuclear ceramics operate under temperature gradients, irradiation, fission-gas generation, transmutation, variable oxygen potential, corrosion, and long-term chemical evolution [10–12]. Many controlling processes are localized at cation sublattices, grain boundaries, bubble–matrix interfaces, precipitates, or radionuclide-hosting phases. This localization suggests a design problem distinct from global compositional mixing: complexity may be useful only at the structural unit that controls a limiting process. We use PLHE for such deliberately localized design. The modified unit must be defined structurally and compositionally, linked to a specific performance limitation, and evaluated against a lower-complexity reference under relevant conditions. Site-selective disorder, complexion engineering, and hierarchical multiphase design provide related concepts. PLHE integrates these ideas around a common nuclear-service objective and validation route.

2. UO_2 as a Fission-Evolved, Compositionally Complex Ceramic

Fresh UO_2 is a fluorite-structured oxide with uranium occupying the cation sublattice and oxygen occupying the anion sublattice. In conventional enriched light-water-reactor fuel, ^{238}U remains the major isotope, whereas ^{235}U is present at a few percent, with the exact enrichment depending on the fuel design and reactor requirements. Two nuclear-reaction pathways are particularly relevant to the in-service compositional evolution of UO_2 fuel. Neutron absorption by ^{235}U produces an excited compound nucleus that can undergo fission:

$$^{235}\mathrm{U} + n \rightarrow {}^{236}\mathrm{U}^{*} \rightarrow \text{fission fragments} + \bar{\nu}\,\mathrm{n} + \text{energy} \quad (1)$$

where $\bar{\nu}$ denotes the mean number of prompt neutrons emitted per fission. In parallel, neutron capture by ^{238}U initiates a breeding sequence:

$$^{238}\mathrm{U} + n \rightarrow {}^{239}\mathrm{U} \xrightarrow{\beta^-} {}^{239}\mathrm{Np} \xrightarrow{\beta^-} {}^{239}\mathrm{Pu} \quad (2)$$

^{239}Pu formed through this sequence is fissile and contributes to further fission and fission-product generation. Equations (1) and (2) continuously change the fuel inventory. The associated chemical redistribution is governed by irradiation source terms, temperature gradients, oxygen-potential variation, solubility limits, redox chemistry, and diffusion kinetics [13–16], producing a non-equilibrium phase-partitioned state. Rare-earth fission products and some actinides can enter UO_2-based solid solutions; Xe and Kr form intra- and intergranular bubbles; and Ru, Rh, Pd, Tc, together with a condition-dependent fraction of Mo, contribute to noble-metal precipitates. Ba-, Sr-, Zr-, Mo-, U-, and O-containing complex oxides can form under appropriate local chemistry. Mo partitioning is particularly sensitive to oxygen potential and can shift between metallic and oxidic states [15,16]. High-burnup restructuring further changes grain size, porosity, defect content, and local chemistry [14,16,17].

SIMFUEL reproduces selected burnup-dependent chemical inventories and representative fission-product states without the radiological constraints of reactor fuel [15,18]. It does not reproduce the complete irradiation-defect population, fission-gas history, in-pile thermal gradient, transmutation sequence, or non-equilibrium kinetics. It is therefore a chemical and microstructural analogue rather than a full surrogate. Post-irradiation examination and high-burnup fuel studies remain necessary to establish phase distributions and local structures [14,16].

Figure 1 summarizes the major product classes and the principal drivers of their partitioning. Burnup, temperature, oxygen potential, radiation-enhanced diffusion, and solubility limits determine whether species remain in matrix solid solution, segregate to grain boundaries, form fission-gas bubbles, precipitate as noble-metal particles, or enter redox-dependent oxide phases.

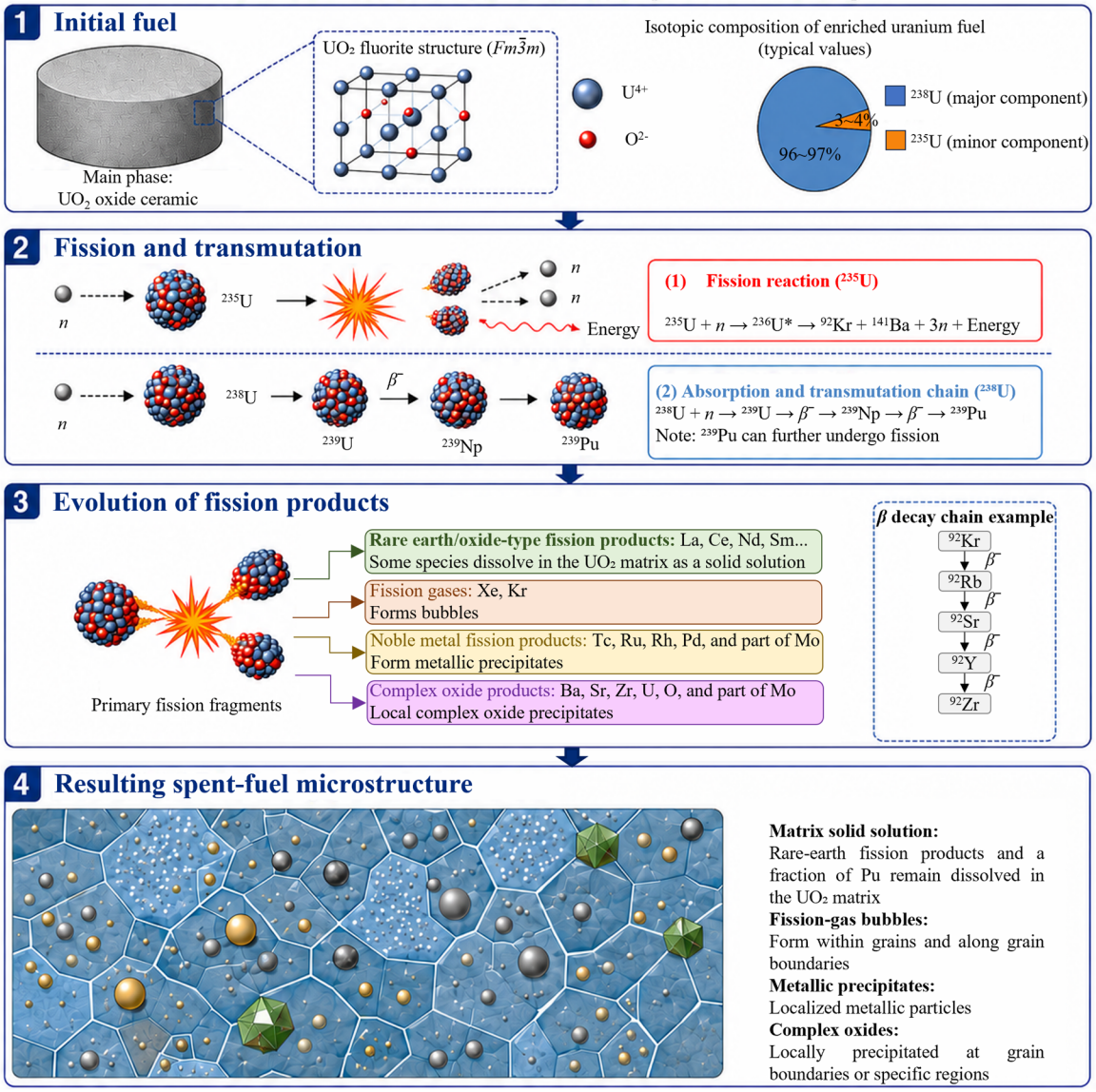


Figure 1. Fission-driven chemical evolution and phase partitioning in UO_2 fuel. The schematic separates matrix solutes, Xe/Kr bubbles, noble-metal precipitates, and complex oxides, with grain-boundary localization indicated in the final microstructure. Burnup, temperature, oxygen potential, radiation-enhanced diffusion, and solubility limits govern the partitioning. The enrichment values and reaction pathways are illustrative.

3. Thermodynamic, Kinetic, and Spatial Classification of Multicomponent Nuclear Ceramics

Spent UO_2 remains U-dominated and most fission products are dilute at the pellet scale. Its irradiation microstructure is therefore better described as a phase-partitioned, non-equilibrium multicomponent state than as a homogeneous high-entropy phase. For the present discussion, four state classes are useful: compositionally complex phases, high-configurational-entropy phases, entropy-stabilized phases, and kinetically retained irradiation-induced heterogeneous states. The last category may contain substantial local chemical complexity while remaining controlled by source terms, diffusion distances, defect sinks, redox gradients, and finite irradiation time rather than equilibrium free-energy minimization.

Here, compositionally complex denotes a multicomponent phase or local environment without demonstrated entropy control. High-configurational-entropy denotes substantial multi-principal occupancy within a phase or on a defined crystallographic sublattice for which configurational entropy is a useful descriptor. Entropy stabilization is a stronger thermodynamic claim that the disordered state must be stabilized relative to competing states by entropy, ideally demonstrated through reversible temperature-dependent phase behavior [1,5,6]. PLHE is orthogonal to these thermodynamic labels: it specifies where complexity is deliberately placed and how the resulting function is evaluated. A PLHE unit may be compositionally complex, high-configurational-entropy, or entropy-stabilized depending on the evidence. Table 1 summarizes the distinctions and minimum evidence.

Table 1. Definitions and minimum evidence for multicomponent and PLHE states.

State	Defining Criterion	Thermodynamic/Kinetic Status	Minimum Evidence
Compositionally complex	Several species share a phase/region; entropy control unproven	Equilibrium or metastable	Quantitative composition + phase constitution
High-configurational-entropy	Multiple principal species occupy a defined sublattice; ΔS_{conf} is substantial	Configurational entropy is substantial; stability not implied	Site occupancy + local composition + phase purity
Entropy-stabilized	Entropy changes phase stability relative to competitors	Equilibrium/reversible thermodynamic criterion	Temperature-dependent reversibility + thermodynamic analysis
Irradiation-induced heterogeneous	Chemically partitioned state maintained by irradiation/gradients/kinetics	Kinetically maintained, non-equilibrium	PIE/local chemistry + defect/kinetic context
PLHE	Complexity deliberately confined to a selected unit and linked to a target function	Orthogonal design label; equilibrium or metastable	Spatial confinement + site occupancy + matched control + service-relevant performance with mechanistic attribution

No universal ΔS_{conf} threshold is imposed here because crystallographic site multiplicities and accessible configurations differ among ceramic structure types; the site-resolved value should therefore be reported for the specific sublattice or local region being classified. For a crystalline phase or locally resolved region α described by a multisublattice model, the ideal configurational-entropy screening descriptor is given by Equation (3):

$$\Delta S_{\mathrm{conf}}^{\alpha,\mathrm{ideal}} = -R \sum_s m_s \sum_i x_{i,s}^{\alpha} \ln x_{i,s}^{\alpha}, \ \sum_i x_{i,s}^{\alpha} = 1 \quad (3)$$

Here, m_s is the number of sites belonging to sublattice s per formula unit and $x_{i,s}^{\alpha}$ is the site fraction of species i on that sublattice. Unequal site multiplicities are handled explicitly by m_s. Vacancies are treated as species when they occupy configurational sites. Oxygen nonstoichiometry is represented on the anion sublattice, and mixed-valence states (for example, U^{4+}/U^{5+}) must be distinguished when they participate in charge compensation. The site fractions must satisfy sublattice normalization and global charge neutrality. Equation (3) is an ideal upper-bound descriptor; short-range order, site correlations, defect–solute coupling, interfacial excesses, and irradiation-driven segregation can lower or otherwise modify the accessible configurational entropy. These effects require diffraction/PDF, spectroscopy, atom-probe or atomic-resolution microscopy, and, where appropriate, cluster-expansion/Monte Carlo or defect-thermodynamic treatment.

For equilibrium screening, the free-energy balance can be written schematically as:

$$\Delta G^{a} = \Delta H_{\mathrm{mix}}{}^{a} + \Delta G_{\mathrm{defect}}{}^{a} + \Delta G_{\mathrm{redox}}{}^{a} + \Delta G_{\mathrm{strain}}{}^{a} - T(\Delta S_{\mathrm{conf}}{}^{a} + \Delta S_{\mathrm{vib}}{}^{a}) \quad (4)$$

Equation (4) is a decomposition of the relevant free-energy contributions rather than a closed predictive model. Entropy stabilization depends on competition among mixing enthalpy, defect and redox energetics, strain, and configurational and vibrational entropy. Under irradiation, ballistic defect production, sinks, radiation-enhanced diffusion, gas generation, and finite-time kinetics introduce additional non-equilibrium constraints. Therefore, a metastable irradiation state cannot be classified from ΔS_{conf} alone. Figure 2 places the principal state classes on a schematic thermodynamic–kinetic map.

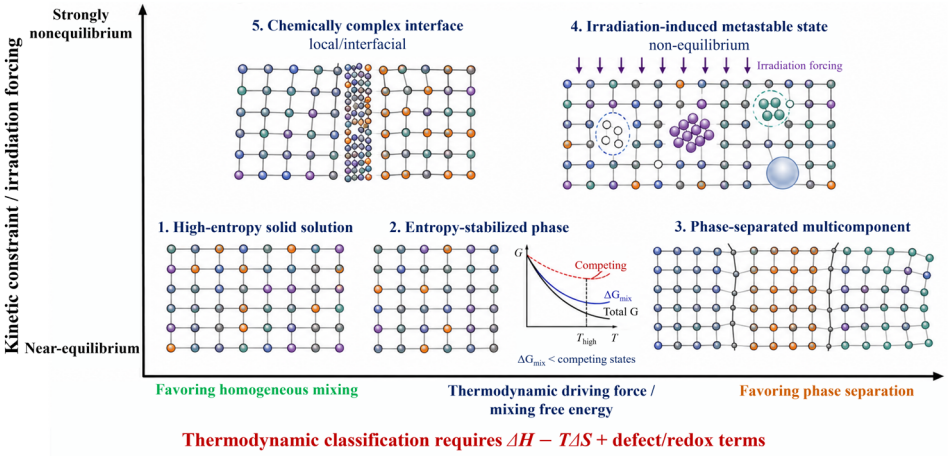


Figure 2. Thermodynamic and kinetic classification of multicomponent nuclear-ceramic states. Homogeneous high-configurational-entropy and entropy-stabilized states are separated from equilibrium phase-separated materials,

irradiation-induced metastable states, and chemically complex interfaces. The diagram is conceptual: thermodynamic classification requires the complete free-energy balance, whereas irradiation states additionally require kinetic and spatially resolved evidence.

4. PLHE as a Selective-Placement Design Framework

PLHE does not define a new thermodynamic state. Its distinction lies in how compositional complexity is allocated and evaluated. The selected unit is a sublattice, grain-boundary region, interface, or secondary phase expected to control a service-limiting process. Its local chemistry and site occupancy are resolved, and its effect is compared with a matched lower-complexity reference. Local high entropy restricts complexity spatially, for example to a grain-boundary zone or interface, whereas partial high entropy restricts it crystallographically or by phase, for example to one sublattice or a secondary host phase. A candidate may satisfy either restriction or both. Accordingly, the PLHE designation rests on resolved confinement and site occupancy rather than nominal composition alone.

Figure 3 summarizes these definitions without assigning a performance benefit to any specific nuclear material. The matrix retains its primary function, while additional compositional freedom is placed only in the unit linked to the target mechanism. Candidate units in nuclear ceramics include a fuel-matrix sublattice, grain-boundary complexion, bubble–matrix interface, or radionuclide-hosting phase.

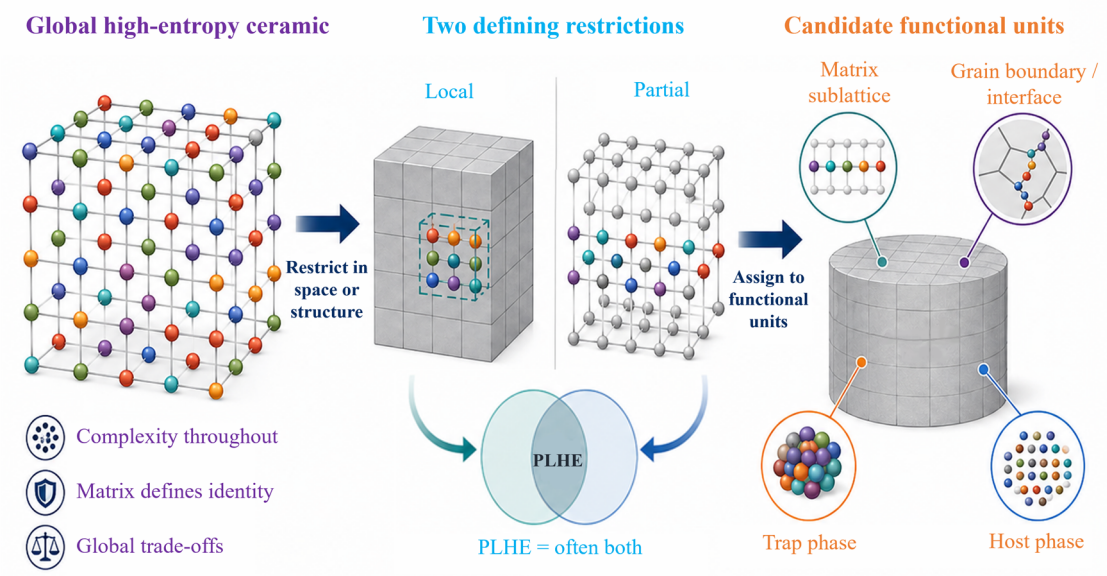


Figure 3. Global, local, partial, and PLHE design. Global high entropy distributes compositional complexity through the material or dominant phase. Local and partial high entropy restrict it in space or to a selected phase, sublattice, compound, or local environment. PLHE combines these restrictions while retaining a conventional matrix.

5. Design Principles and Constraints

5.1. Preserve the Primary Matrix Function

The matrix should first satisfy the fundamental requirements of the application. For a fuel, these include actinide density, thermal transport, oxygen-potential compatibility, phase stability, manufacturability, fuel–cladding compatibility, and reactor-specific neutronics. For a waste form, they include waste loading, chemical durability, radiation tolerance, processability, and long-term phase stability [19]. Complexity should not be introduced simply because a larger composition space is available. It is justified only when it improves a defined function without imposing an unacceptable penalty elsewhere.

5.2. Identify the Controlling Bottleneck

PLHE design should start from a specific performance limit rather than a target entropy value. In oxide fuels, relevant limits include thermal-conductivity degradation, fission-gas swelling and release, grain-boundary weakening, fission-product redistribution, and interfacial chemical attack. In waste forms, they include variable waste inventories, actinide retention, aqueous corrosion, radiation-induced amorphization, helium accumulation, and phase incompatibility. The selected unit should have a direct mechanistic link to the limiting process.

5.3. Couple Phase Partitioning with Defect Chemistry

Nuclear oxides are multisublattice defect systems. Aliovalent substitution can change oxygen-vacancy populations, actinide valence, charge compensation, diffusion, redox equilibria, and phase stability. Candidate PLHE compositions must therefore be evaluated using coupled cation–anion defect chemistry under realistic oxygen potentials. Ideal configurational entropy alone is insufficient because charge imbalance, local bonding, or competing ordered phases may destabilize the target structure [20].

5.4. Use an Application-Specific Reference

PLHE candidates should be compared with a lower-complexity reference prepared with comparable processing, density, grain size, defect content, and phase constitution. Without such control, differences may arise from porosity, secondary phases, dopant chemistry, or microstructural refinement rather than selective complexity. The relevant measure is the net mechanistic benefit after these variables are separated.

5.5. Specify the Radiation-Response Metric

Radiation tolerance encompasses several distinct responses. In nuclear ceramics, relevant metrics include resistance to amorphization, limited defect accumulation, dynamic recovery, suppression of irradiation-induced segregation, gas-bubble evolution and swelling, radionuclide retention, and resistance to radiation-enhanced dissolution [21–26]. These responses are not interchangeable: resistance to amorphization, for example, does not ensure favorable cation redistribution or aqueous durability. Chemical complexity can also introduce countereffects through local strain, reduced defect mobility and recombination, stronger He or fission-gas trapping, irradiation-induced phase separation, radiation-enhanced diffusion, or segregation of redox-active and volatile species. PLHE studies should therefore define the relevant damage metric and mechanism explicitly rather than use radiation tolerance as a generic outcome.

6. Application-Specific Opportunities, Constraints, and Maturity

6.1. Near-Term Opportunity: Compositionally Complex Waste-Form Ceramics

Waste-form ceramics provide the most direct near-term setting in which to test PLHE concepts because their primary function is radionuclide immobilization rather than heat generation or neutron economy. Candidate hosts include defect fluorite, pyrochlore, zirconolite, murataite, garnet, apatite, hollandite, and perovskite-related ceramics. Their distinct crystallographic sites can accommodate actinides, rare-earth fission products, Cs/Ba, Sr, and transition-metal species through size/valence matching and charge compensation [19,25,27–29]. Compositionally complex variants may broaden selected solubility windows or accommodate variable waste inventories, but increased elemental diversity alone does not establish improved durability or irradiation response. Table 2 relates representative host families to the target species, modified unit, intended mechanism, lower-complexity control, and validation metric.

A multiphase waste form may be compositionally complex at the material scale even when each phase has low configurational entropy. The term high-entropy waste form is therefore appropriate only when multiple principal species occupy a defined sublattice within the relevant host phase. For many waste streams, a deliberately multiphase ceramic may be more suitable than a single high-entropy phase because different radionuclides favor different crystal-chemical hosts.

6.2. Waste Forms as a Nearer-Term Technical Route

The design spaces of waste forms and fuels are fundamentally different. Waste forms prioritize radionuclide incorporation, aqueous durability, radiation response, phase stability, tolerance to variable waste inventories, and long-term chemical evolution. Fuels must additionally preserve fissile/heavy-metal density, thermal conductivity and melting margin, fission-gas behavior, swelling and restructuring, fuel–cladding chemical compatibility, reactor physics, fabrication, and ultimately licensing. A composition that performs well as a durable waste host can therefore be unsuitable as a fuel even when its local irradiation response is favorable. The fuel-related cases below are consequently treated as screening problems in which any local benefit must be weighed against these system-level penalties.

Table 2. Candidate PLHE waste-form systems and validation metrics.

Host Family	Target Species/Class	PLHE Unit	Target Function/Mechanism	Matched Control	Key Validation
Pyrochlore/defect fluorite	Actinides, rare earths	A/B cation sublattice or disorder domain	Site accommodation; disorder/amorphization response	Single-/few-cation analogue	Site occupancy; critical amorphization dose; leaching
Zirconolite/Synroc	Pu/minor actinides, RE fission products	Ca/Zr/Ti sites within selected phase	Partition radionuclides into durable host	Conventional zirconolite/Synroc phase	Phase fraction; actinide loading; leaching; α-decay/He
Hollandite	Cs/Ba	Tunnel + framework-cation chemistry	Cs retention and charge compensation	Lower-complexity titanate hollandite	Cs site occupancy; EXAFS; aqueous release
Apatite/garnet/murataite	Actinides/lanthanides (system dependent)	Selected cation sublattice	Flexible charge/size accommodation	Binary/ternary host of same structure	Phase stability; solubility; irradiation response
Perovskite-related	Actinides/lanthanides	A/B sites with vacancy control	Controlled defect chemistry and amorphization response	Single-dopant perovskite	Vacancy/site occupancy; amorphization; leaching

6.3. Longer-Term Opportunity: Selectively Complex Fuel-Matrix Sublattices

Compositionally complex fluorite oxides demonstrate that cation disorder, ordering transitions, aliovalent substitution, and oxygen vacancies can be tuned over broad composition ranges [7,8,20]. These results justify exploring selective complexity in UO_2-, ThO_2-, or mixed-actinide matrices, but they do not establish the same response in actinide fuels. Possible effects include changes in fission-product solubility, defect association, and phase stability. At the same time, compositionally complex fluorites often have reduced thermal conductivity because cation-mass disorder, local strain, force-constant variation, and oxygen vacancies increase phonon scattering [7,9,30]. This behavior is useful for thermal-barrier applications but imposes a thermal penalty in nuclear fuels. Fuel design should therefore use the minimum local or partial complexity needed for a defined benefit while preserving heat removal and heavy-metal density.

When a non-actinide cation substitutes on the U/actinide sublattice, heavy-metal and fissile-atom number densities are diluted approximately in proportion to the substituted site fraction before lattice-parameter and density changes are considered. The actual penalty depends on dopant concentration and mass, oxidation state and charge compensation, theoretical density and porosity, lattice parameter, and whether substitution occurs on the actinide sublattice or is accommodated through oxygen-related defects. Neutronic consequences are likewise isotope- and spectrum-dependent. To illustrate the scale of the site-dilution effect, Table 3 presents a sensitivity calculation for $U_{1-x}M_xO_2$ with 4 at.% ^{235}U in the uranium inventory and fixed cation-site density. M is assigned $\sigma_a = 1$ barn to separate the dilution effect from the chemistry of a strong neutron absorber. The normalized values are not a reactor-physics prediction. They show the first-order change in heavy-metal/fissile density and in a thermal-absorption proxy before lattice, porosity, spectrum, and depletion effects are included. Candidate compositions would require transport/depletion calculations, activation and transmutation inventories, measured density/porosity, thermal conductivity, phase and melting margins, oxygen potential, fabrication behavior, and fuel–cladding compatibility [31,32].

Table 3. Illustrative sensitivity analysis for cation-site substitution in $U_{1-x}M_xO_2$.

x in $U_{1-x}M_xO_2$	Normalized HM Cation Density	Normalized ^{235}U Atom Density	Normalized Thermal Absorption Proxy *	Interpretation
0	1.00	1.00	1.000	Reference UO_2
0.05	0.95	0.95	0.952	5% reduction in HM and fissile atom density
0.10	0.90	0.90	0.903	10% reduction in HM and fissile atom density
0.20	0.80	0.80	0.807	20% reduction in HM and fissile atom density

* The absorption proxy uses $\sigma_{a,\,eff}(U) = 0.04\sigma_a(^{235}U) + 0.96\sigma_a(^{238}U)$ and $\sigma_a(M) = 1$ barn. Cation-site density is fixed and all values are normalized to UO_2. This is a sensitivity calculation, not a reactor model. Thermal cross sections for uranium are from NIST [33].

6.4. Exploratory Opportunity: Grain-Boundary and Interface Chemistry

Grain boundaries participate in fission-gas bubble nucleation and interconnection, intergranular fracture, solute segregation, and oxygen transport [10,14,16]. In Cr-doped UO_2, segregation and precipitation at grain boundaries vary with dopant level [31], illustrating why local chemistry must be resolved rather than inferred from nominal composition. Multicomponent boundary chemistry could alter defect absorption, bubble evolution, or solute redistribution, but it could also promote fast interfacial diffusion, connected porosity, gas trapping, or mechanically weak boundary films. Evaluation therefore requires boundary-resolved chemistry, in situ or post-irradiation bubble analysis, and interface-specific mechanical or transport measurements.

6.5. Exploratory Opportunity: Compositionally Complex Trap or Sink Phases

Spent UO_2 contains noble-metal particles and complex oxides formed by phase partitioning during irradiation. This behavior suggests that engineered sink phases could be explored for selected fission products or defects. Candidate families include fluorite-, pyrochlore-, perovskite-, zirconolite-, and related complex oxides [20,29,34,35]. Their use inside a fuel pellet would depend on phase compatibility, coarsening, thermal resistance, oxygen-potential coupling, swelling, and neutronic effects. At present, such concepts are better described as compositionally complex trap or sink phases unless multi-principal site occupancy and an entropy-based role are established.

7. Research and Validation Roadmap

Figure 4 translates the concept into two application tracks. Track A covers compositionally complex waste forms, for which host families and durability metrics are established. Track B covers fuel matrices, interfaces, and in-fuel sink phases. Fuel-related concepts require thermal, redox, phase-compatibility, and reactor-specific neutronic screening before irradiation testing.

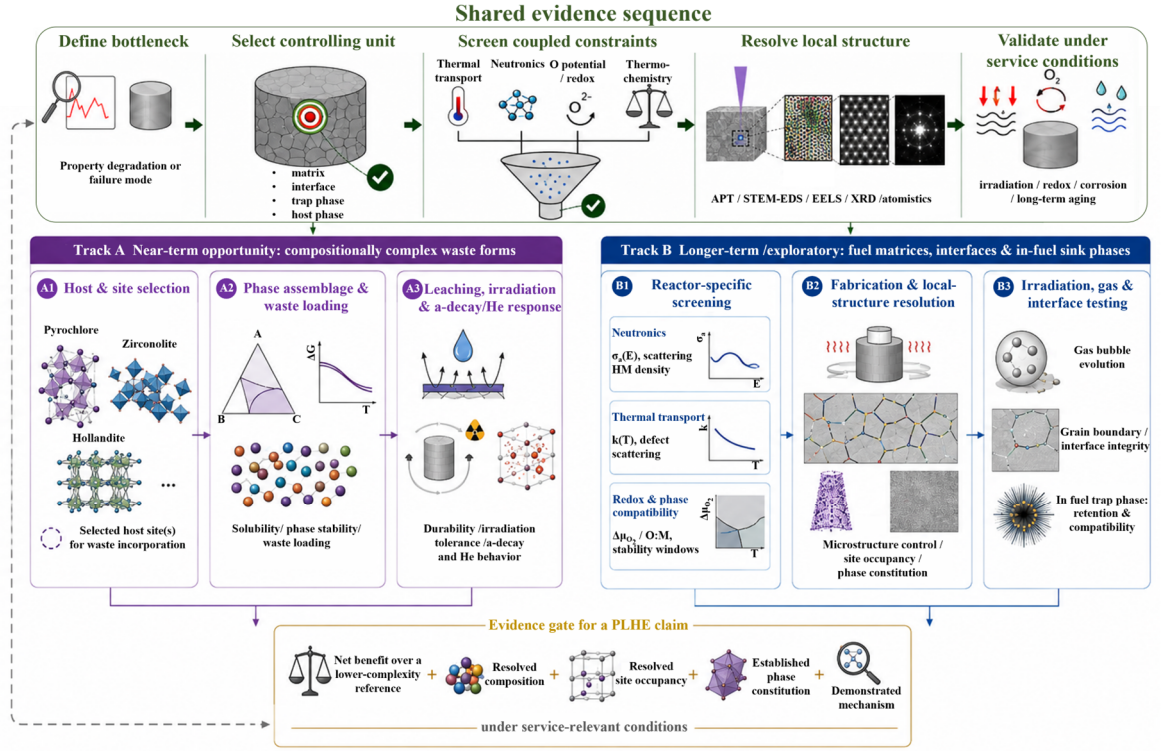


Figure 4. Research and validation pathway for fission-informed PLHE nuclear ceramics. Near-term waste-form concepts and longer-term fuel/interface/sink concepts converge on a common evidence gate requiring quantitative composition and phase constitution, resolved spatial confinement/site occupancy, a closely matched lower-complexity control, and service-relevant performance with mechanistic attribution.

Both tracks follow the same sequence: define the bottleneck, select the controlling unit, screen coupled constraints, resolve local structure, and test under service-relevant conditions. The evidence gate in Figure 4 is defined in measurable terms. Composition and phase constitution must be quantified, spatial confinement and site occupancy must be resolved, the lower-complexity reference should be matched as closely as possible in density, porosity, grain size, actinide loading, phase fraction, and processing history, and the target property should be

measured under relevant thermal, chemical, and irradiation conditions. Evidence based only on room-temperature phase identification or qualitative microscopy is insufficient because the PLHE claim concerns a specified local unit and its service response. Mechanistic attribution should therefore combine microscopy and spectroscopy with thermodynamic, atomistic, kinetic, or reactor-physics modelling as appropriate.

8. Outlook

The phase-partitioned chemistry of irradiated UO_2 reveals a hierarchy of chemically active length scales—from matrix sublattices and grain boundaries to gas bubbles, metallic precipitates, and complex oxides—at which defect populations, redox state, and composition are coupled. PLHE uses this hierarchy as a design principle by introducing compositional complexity selectively at units that control target functions while preserving the primary role of the surrounding matrix.

Waste-form hosts provide the clearest near-term route because site-selective radionuclide incorporation is already central to their crystal chemistry. Fuel matrices, grain boundaries, and in-fuel sink phases are longer-term directions because thermal transport, neutronics, oxygen potential, and irradiation kinetics impose coupled constraints. Progress will depend on resolved site occupancy, controlled lower-complexity references, and direct evidence linking the modified unit to performance under service-relevant conditions.

The useful design variable is therefore not nominal entropy alone, but the amount and location of compositional complexity required for a measurable nuclear-material function.

Author Contributions

J.W.: investigation, data curation, writing—original draft preparation, visualization; Y.Z.: conceptualization, supervision, writing—reviewing and editing. Both authors have read and agreed to the published version of the manuscript.

Funding

This work was supported by the National Natural Science Foundation of China (Grant No. 52273280).

Institutional Review Board Statement

Not applicable.

Informed Consent Statement

Not applicable.

Data Availability Statement

Dataset available on request from the authors.

Conflicts of Interest

Given the role as the Editor-in-Chief, Yong Zhang had no involvement in the peer review of this paper and had no access to information regarding its peer-review process. Full responsibility for the editorial process of this paper was delegated to another editor of the journal.

Use of AI and AI-Assisted Technologies

During the preparation of this work, the authors used OpenAI ChatGPT 5.6 Sol to assist with language polishing and to improve the quality of Figures. No experimental images or quantitative data were generated or altered by AI tools. After using this tool, the authors reviewed and edited the content as needed and take full responsibility for the content of the published article.

References

1. Rost, C.M.; Sachet, E.; Borman, T.; et al. Entropy-Stabilized Oxides. *Nat. Commun.* **2015**, *6*, 8485. https://doi.org/10.1038/ncomms9485.
2. Jiao, Y.; Dai, J.; Fan, Z.; et al. Overview of High-Entropy Oxide Ceramics. *Mater. Today* **2024**, *77*, 92–117. https://doi.org/10.1016/j.mattod.2024.06.005.

3. Dube, T.C.; Zhang, J. Underpinning the Relationship between Synthesis and Properties of High Entropy Ceramics: A Comprehensive Review on Borides, Carbides and Oxides. *J. Eur. Ceram. Soc.* **2024**, *44*, 1335–1350. https://doi.org/10.1016/j.jeurceramsoc.2023.10.023.
4. Luo, J. From High-Entropy Ceramics to Compositionally Complex Ceramics and Beyond. *J. Materiomics.* **2026**, *12*, 101173. https://doi.org/10.1016/j.jmat.2026.101173.
5. Musicó, B.L.; Gilbert, D.; Ward, T.Z.; et al. The Emergent Field of High Entropy Oxides: Design, Prospects, Challenges, and Opportunities for Tailoring Material Properties. *APL Mater.* **2020**, *8*, 040912. https://doi.org/10.1063/5.0003149.
6. Brahlek, M.; Gazda, M.; Keppens, V.; et al. What Is in a Name: Defining "High Entropy" Oxides. *APL Mater.* **2022**, *10*, 110902. https://doi.org/10.1063/5.0122727.
7. Gild, J.; Samiee, M.; Braun, J.L.; et al. High-Entropy Fluorite Oxides. *J. Eur. Ceram. Soc.* **2018**, *38*, 3578–3584. https://doi.org/10.1016/j.jeurceramsoc.2018.04.010.
8. Wright, A.J.; Luo, J. A Step Forward from High-Entropy Ceramics to Compositionally Complex Ceramics: A New Perspective. *J. Mater. Sci.* **2020**, *55*, 9812–9827. https://doi.org/10.1007/s10853-020-04583-w.
9. Wright, A.J.; Wang, Q.; Huang, C.; et al. From High-Entropy Ceramics to Compositionally-Complex Ceramics: A Case Study of Fluorite Oxides. *J. Eur. Ceram. Soc.* **2020**, *40*, 2120–2129. https://doi.org/10.1016/j.jeurceramsoc.2020.01.015.
10. Olander, D.R. *Fundamental Aspects of Nuclear Reactor Fuel Elements*; Technical Information Center, Office of Public Affairs, Energy Research and Development Administration: Oak Ridge, TN, USA, 1976. https://doi.org/10.2172/7343826.
11. Weber, W.J.; Ewing, R.C.; Catlow, C.R.A.; et al. Radiation Effects in Crystalline Ceramics for the Immobilization of High-Level Nuclear Waste and Plutonium. *J. Mater. Res.* **1998**, *13*, 1434–1484. https://doi.org/10.1557/jmr.1998.0205.
12. Ewing, R.C. Long-Term Storage of Spent Nuclear Fuel. *Nat. Mater.* **2015**, *14*, 252–257. https://doi.org/10.1038/nmat4226.
13. Kleykamp, H. The Chemical State of the Fission Products in Oxide Fuels. *J. Nucl. Mater.* **1985**, *131*, 221–246. https://doi.org/10.1016/0022-3115(85)90460-x.
14. Ge, Z.; Yan, D.; Lei, P.; et al. A Comprehensive Review of High Burn-up Structure Formation in UO_2: Mechanisms, Interactions, and Future Directions. *Nanomaterials* **2025**, *15*, 325. https://doi.org/10.3390/nano15050325.
15. Lucuta, P.G.; Verrall, R.A.; Matzke, H.; et al. Microstructural Features of SIMFUEL—Simulated High-Burnup UO_2-Based Nuclear Fuel. *J. Nucl. Mater.* **1991**, *178*, 48–60. https://doi.org/10.1016/0022-3115(91)90455-g.
16. Matzke, H. On the Rim Effect in High Burnup UO_2LWR Fuels. *J. Nucl. Mater.* **1992**, *189*, 141–148. https://doi.org/10.1016/0022-3115(92)90428-n.
17. Barker, M.A.; Adam, M.S.; Little, P.; et al. Observations of High Burnup Structure in AGR Fuel. *Prog. Nucl. Energy* **2022**, *153*, 104433. https://doi.org/10.1016/j.pnucene.2022.104433.
18. Kim, D.J.; Yang, J.H.; Kim, J.H.; et al. Effects of Solid Fission Products Forming Dissolved Oxide (Nd) and Metallic Precipitate (Ru) on the Thermal Conductivity of Uranium Base Oxide Fuel. *Thermochim. Acta* **2007**, *455*, 123–128. https://doi.org/10.1016/j.tca.2006.12.005.
19. Pilania, R.K.; Dube, C.L. Matrices for Radioactive Waste Immobilization: A Review. *Front. Mater.* **2023**, *10*, 1236470. https://doi.org/10.3389/fmats.2023.1236470.
20. Chen, K.; Pei, X.; Tang, L.; et al. A Five-Component Entropy-Stabilized Fluorite Oxide. *J. Eur. Ceram. Soc.* **2018**, *38*, 4161–4164. https://doi.org/10.1016/j.jeurceramsoc.2018.04.063.
21. Huang, S.; Zhang, J.; Fu, H.; et al. Irradiation Performance of High Entropy Ceramics: A Comprehensive Comparison with Conventional Ceramics and High Entropy Alloys. *Prog. Mater. Sci.* **2024**, *143*, 101250. https://doi.org/10.1016/j.pmatsci.2024.101250.
22. Xu, L.; Su, L.; Niu, M.; et al. Irradiation Induced Structural Damage and Evolution of Mechanical Properties in High Entropy Fluorite Oxide. *J. Eur. Ceram. Soc.* **2023**, *43*, 3507–3515. https://doi.org/10.1016/j.jeurceramsoc.2023.02.003.
23. Daghbouj, N.; AlMotasem, A.T.; Li, B.; et al. Defect Landscape Engineering Suppresses Helium Damage in Ceramics. *Commun. Mater.* **2026**, *7*, 97. https://doi.org/10.1038/s43246-026-01083-3.
24. Bae, I.T.; Weber, W.J.; Ishimaru, M.; et al. Effect of Ionization Rates on Dynamic Recovery Processes during Electron-Beam Irradiation of 6*H*-SiC. *Appl. Phys. Lett.* **2007**, *90*, 121910. https://doi.org/10.1063/1.2715135.
25. Xu, X.; Ning, X.; Dong, F.; et al. Low Temperature Fabrication of $Ba_{0.9}Cs_{0.3}Cr_{2.1}Ti_{5.9}O_{16}$ Ceramic Waste Form for Cesium Immobilization Using Bi_2O_3 as Sintering Aid. *Chem. Eng. J.* **2024**, *492*, 152166. https://doi.org/10.1016/j.cej.2024.152166.
26. Daghbouj, N.; AlMotasem, A.T.; Duchoň, J.; et al. Nanoscale Strain Evolution and Grain Boundary-Mediated Defect Sink Behavior in Irradiated SiC: Insights from N-PED and DFT. *Acta Mater.* **2026**, *303*, 121739. https://doi.org/10.1016/j.actamat.2025.121739.
27. Sickafus, K.E.; Minervini, L.; Grimes, R.W.; et al. Radiation Tolerance of Complex Oxides. *Science* **2000**, *289*, 748–751. https://doi.org/10.1126/science.289.5480.748.
28. Wang, Y.; Jing, C.; Ding, Z.Y.; et al. The Structure, Property, and Ion Irradiation Effects of Pyrochlores: A Comprehensive Review. *Crystals* **2023**, *13*, 143. https://doi.org/10.3390/cryst13010143.

29. Blackburn, L.R.; Corkhill, C.L.; Hyatt, N.C. A Review of Zirconolite Solid Solution Regimes for Plutonium and Candidate Neutron Absorbing Additives. *Ceramics* **2023**, *6*, 1330–1347. https://doi.org/10.3390/ceramics6030082.
30. Braun, J.L.; Rost, C.M.; Lim, M.; et al. Charge-Induced Disorder Controls the Thermal Conductivity of Entropy-Stabilized Oxides. *Adv. Mater.* **2018**, *30*, 1805004. https://doi.org/10.1002/adma.201805004.
31. Terricabras, A.J.; Galvin, C.O.T.; Kosmidou, M.; et al. Chromium Doping Effects on UO_2 Grain Boundary Chemistry: A Combined Experimental and Modeling Approach. *J. Nucl. Mater.* **2025**, *617*, 156114. https://doi.org/10.1016/j.jnucmat.2025.156114.
32. Alshannaq, M.; Owen, C.; Ferrigno, J.; et al. Implications of Point Defect Accumulation on UO_2 Thermal Conductivity and Fission Gas Release under Accelerated Fuel Irradiation. *J. Nucl. Mater.* **2025**, *616*, 156057. https://doi.org/10.1016/j.jnucmat.2025.156057.
33. NIST Center for Neutron Research. Neutron Scattering Lengths and Cross Sections. Available online: https://www.nist.gov/ncnr/planning-your-experiment/scattering-length-periodic-table (accessed on 2 September 2026).
34. Ko, S.T.; Lee, T.; Qi, J.; et al. Compositionally Complex Perovskite Oxides: Discovering a New Class of Solid Electrolytes with Interface-Enabled Conductivity Improvements. *Matter* **2023**, *6*, 2395–2418. https://doi.org/10.1016/j.matt.2023.05.035.
35. Wang, Z.; Zhou, L.; Liu, C.; et al. The Irradiation Resistance and Mechanical Properties of the High-Entropy Zirconate Pyrochlore $(La_{0.2}Nd_{0.2}Sm_{0.2}Eu_{0.2}Gd_{0.2})_2Zr_2O_7$. *Nucl. Instrum. Methods Phys. Res. Sect. B Beam Interact. Mater. Atoms* **2024**, *549*, 165285. https://doi.org/10.1016/j.nimb.2024.165285.